THE IMPACT OF DEPOSITION PARAMETERS ON THE THERMAL CONDUCTIVITY OF CVD THIN DIAMOND FILMS

John A. Herb, Carey Bailey and K.V. Ravi
Crystallume
125 Constitution Dr., Menlo Park, CA 94025

Paul A. Dennig
Materials Science Dept.
Stanford University, Stanford, CA 94305

Diamond films fabricated by PECVD have measured thermal conductivities over twice that of copper. This high thermal conductivity together with the other unique properties of diamond films make this material very attractive for a wide range of thermal management applications. In this work we report on the thermal conductivity of diamond films synthesized by D.C. and microwave assisted CVD. The films were characterized by Raman Spectroscopy and Scanning Electron Microscopy. The thermal conductivity was correlated to the methane concentration, the Full Width at Half Maximum (FWHM) of the 1331 cm^{-1} diamond peak of the Raman Spectra, and the ratio of diamond bonds to disordered carbon bonds (Sp^3/Sp^2) taken from the Raman data.

Introduction

Diamond has the highest known thermal conductivity at temperatures around 100°C. It is nearly 3 times better than the best metals and is over 10 times greater than some of the commonly used electrical insulators (Table 1).

Table 1. Thermal Conductivity of Selected Materials at 100°C (W/cm- °K)

Natural Diamond (max.)	14.0
CVD Diamond	10.0-13.0
Electrical Conductors	
Silver	4.3
Copper	4.0
Graphite	2.1
Electrical Insulators	
SiC	2.7
Beryllium Oxide	2.2
AlN	1.7
Al_2O_3	0.4
Sapphire	0.3

In conjunction with its very high thermal conductivity, diamond also possesses other unique properties such as chemical inertness, high electrical resistivity and extreme

conductivity and intrinsic film parameters independent of detailed deposition conditions. An additional goal was to determine if it was possible to achieve a thermal conductivity greater than 10 W/cm-°C by fabricating a film at 0.05% methane.

Measurement Method

The technique used to measure thermal conductivities in this study is a radiation cooling method first developed for thin films by Ono and co-workers[7]. This method uses radiation thermometry to measure the temperature of a thin film, heated at its ends, whose only heat loss mechanism is blackbody radiation to its surrounding. Analysis of the heat balance equations in this situation gives the following expression for the temperature along the length of the film in terms of the thermal conductivity, λ:

$$T(x) = \{(T_m^4 - T_s^4)/4T_m^3\}[\cosh(kx) - 1] + T_m \qquad (1)$$

$$\text{where } k = (8esT_m^3/\lambda t)^{1/2}$$

T_m= Minimum temperature along the film t = Film thickness
x = Position along the length of the film s = Stefan Boltzmann Constant
e = Total film hemispherical emissivity T_s= Temperature of the surroundings

Inverting equation 1 gives an expression from which the thermal conductivity can be calculated by knowing the temperature profile along the film, the temperature of the immediate sample surroundings, the film thickness and the emissivity of the film.

$$\lambda = 8esT_m^3x^2/t\{\text{arc cosh}[4T_m^3(T-T_m)/(T_m^4-T_s^4)+1]\}^2 \qquad (2)$$

The sample to be tested was suspended between two heating posts as shown in figure 1. The sample surfaces were painted with a black paint in order to define the emissivity of the sample. Tests were run to calibrate the emissivity of the paint, typically 0.9, and to check its reproducibility. Thermocouples located in the post adjacent to the film allowed in situ tests of the temperature measurement.

A schematic diagram of the measurement system is shown in figure 2. The experimental cell is designed to heat the sample in vacuum thus preventing any conductive or convective heat losses from the air, and at the same time surround the sample within an enclosure of uniform and known temperature. The infrared detector was focused on the sample through a small slot in the enclosure surrounding the sample. By scanning the detector along the length of the film, a temperature profile similar to that drawn in figure 1 was obtained. The thermal conductivity was calculated from equation 2 from the measured temperature profile of the film.

To test the accuracy of this technique, the thermal conductivities of thin film samples of copper and nickel were measured and compared to published values[9]. As seen in table 2, the deviation varied from about 4% to 16%. The main contribution to the inaccuracy of both the calibration samples and the diamond films was inexact knowledge of the sample thickness. In the case of the metal films, the sample thickness could change due to plastic deformation during sample preparation. For the diamond samples, the films

were sufficiently thin (~2μ) that a thickness variation of .1μ to .2μ can lead to uncertainties of about 10%

Table 2 Thermal Conductivities of Copper and Nickel Calibration Samples.

		Thermal Conductivity (W/cm-°C)		
Material	Thickness	Measured	Literature	Deviation
Copper #1	15μ	3.61	3.98	-9.30%
Copper #2	5μ	4.48	3.98	12.60%
Copper #3	7.9μ	3.44	3.98	-13.60%
Nickel #1	12μ	1.04	0.899	15.70%
Nickel #2	12μ	0.86	0.899	-4.30%

Diamond Deposition Matrix

The matrix of deposition conditions chosen for this investigation is listed in table 3. Two different deposition techniques were used, microwave enhanced CVD and D.C. enhanced CVD. Methane concentrations were varied for each of the techniques and were chosen so that results from the D.C. and microwave systems could be compared at 0.3%. Pressure in the D.C. depositions were varied so that films of 0.3% methane and different pressures could be compared. The deposition temperatures of the microwave samples could not be accurately measured so the numbers listed below are the microwave power in Watts incident on the samples and sample holder. No significant differences in temperature among the microwave depositions should occur with the small power variations that occurred.

Table 3 Diamond Deposition Conditions.

Deposition	% Methane	Temp. °C	Press. (Torr)	Plasma
9-W-35	0.5	725	30	D.C.
1-Q-46	0.3	725	30	D.C.
1-V-43	0.3	725	25	D.C.
6-A-35	0.2	725	45	D.C.
10-N-107	0.3	910 W	50	Microwave
10-N-83	0.1	992 W	50	Microwave
10-N-111	0.1	988 W	50	Microwave
10-N-106	0.05	915 W	50	Microwave

Diamond films for these experiments were deposited directly onto silicon wafers, which were then cut to the desired dimensions or deposited on pieces of silicon already cut to size. The silicon was completely removed in a standard Nitric-HF acid etch and the diamond film mounted in the holder for coated with the black paint. Thickness measurements were made by Scanning Electron Microscopy of the film crossection. Whenever possible, the thickness of the actual test sample was measured. Otherwise, unused pieces of diamond taken from areas adjacent to the sample were measured and that thickness assigned to the sample. A similar method was followed in taking the Raman Spectra. The surface morphology of each film was also examined by SEM.

Figures 3 and 4 show the Raman data of the microwave and D.C. films respectively. All the spectra show a peak near 1331 cm^{-1} characteristic of the Sp^3 bonds of the diamond structure, although with considerable variation of peak width and height. The broad features in the data between 1500 and 1600 cm^{-1} and around 1340 cm^{-1} can be

attributed to disordered Sp^2 bonded carbon[10,11], located at crystallite grain boundaries or possibly within the crystallites. It is clear when comparing microwave and D.C. films deposited at the same methane concentration that the microwave film has a more pronounced diamond character. When grouped together by deposition technique, the data follows the trend typically seen with diamond films; films grown at higher methane concentrations exhibit more Sp^2 structure in the Raman Spectra. In figure 4, comparing D.C. films deposited at 0.3% the one deposited at higher pressure has a more distinguishable diamond peak.

As a way of quantifying the relative amounts of diamond and non-diamond carbon in the films, the Full Width at Half Maximum (FWHM) of the 1331 cm^{-1} peak and a ratio of Sp^3 to Sp^2 has been calculated for each Raman Spectrum in figures 3 and 4. As the amount of disordered carbon decreases in the films, the FWHM will approach that of natural diamond and Sp^3/Sp^2 will be come very large. The FWHM is obtained by expanding the the 1331 cm^{-1} peak of each deposition sufficiently to measure the peak width accurately. The Sp^3/Sp^2 is defined as the ratio of the 1331 cm^{-1} peak height to the maximum peak height in the vicinity of 1580 cm^{-1}, once the luminescent background has been subtracted.

SEM micrographs of the surface morphologies of the microwave films can be seen in figure 5 and those of the D.C. films in figure 6. The microwave films show the typical faceted structure seen in diamond deposited by this method. The mean feature size is approximately 1μ to 2μ. No obvious differences are apparent between films deposited at different methane concentrations. There are clear differences among the D.C. films in figure 6. The lowest methane film of this group has a highly faceted structure similar to the microwave films but with a typical feature size 5 to 10 times smaller. As the methane concentration is increased in the D.C. films, the surface features become smaller and more rounded.

Thermal Conductivity in Diamond Films

Table 4 gives the thermal conductivity of each film along with the deposition parameters, FWHM, Sp^3/Sp^2, and the minimum film temperature, T_m, during the thermal conductivity measurement. Included for reference is the FWHM and the thermal conductivity of natural diamond at 100°C. The two values listed for the thermal conductivity of 1-V-43 and 10-N-107 are the results of separate measurements on two different samples from the same deposition. No accurate value for the FWHM of 9-W-35 could be determined due to lack of a well defined 1331 cm^{-1} peak.

Inspection of table 4 reveals a number of important points. The highest thermal conductivity measured, 12.3 W/cm-°C at 117°C, is very close to that of type IIa diamond measured at the same temperature, 13 W/cm-°C. Clear differences in thermal conductivity exist among the films deposited at 0.3% methane, while no significant difference is observed between microwave films deposited at 0.1% and 0.05% methane. This is illustrated in figure 7 where the methane concentration is plotted against the methane concentration. Included in this figure is similar data taken from reference 7. While the overall trend is similar, the D.C. data appears shifted to lower thermal conductivity values than that of the microwave films. The data from the microwave depositions of reference 7

appears to agree well with the corresponding data from this work. If the methane dependence seen here can be extrapolated to very low methane concentrations, it would suggest that measurable differences could be detected between films deposited at 0.1% and 0.05% methane. No such differences are observed in this data.

Table 4. Thermal Conductivity of Diamond Films.

Deposition	Methane (%)	Pressure (Torr)	FWHM (cm^{-1})	Sp^3/Sp^2	T.C. (W/cm-°C)	Tm (°C)
IIa Nat. Diamond	-	-	3.3	-	14	100
10-N-106	0.05	50	4.6	22.7	11.3	99
10-N-83	0.1	50	6.9	20.3	12.3	117
10-N-111	0.1	50	7.4	20.6	11.0	86.9
10-N-107	0.3	50	10.9	3.3	5.6/5.4	89
6-A-35	0.2	45	10.4	2.4	5.3	70.3
1-Q-46	0.3	30	11.5	1.29	4.4	70
1-V-43	0.3	25	12.2	1.03	3.6/3.8	82
9-W-35	0.5	30	-	0.73	3	73.3

In contrast to what is seen in figure 7, the thermal conductivity correlates with Sp^3/Sp^2 and the FWHM independently of deposition conditions. In figure 8, a plot of thermal conductivity versus Sp^3/Sp^2 results in a monotonic curve with no obvious dependence on pressure, methane or deposition technique. Using the Raman Spectra of reference 7, approximate values of Sp^3/Sp^2 have been calculated and are also plotted in figure 8. A line has been added as an aid to the eye. Both sets of data follow a similar curve and appear to approach an asymptote below the thermal conductivity value at 100°C of a type IIa natural diamond.

Figure 9 is a graph of thermal conductivity as a function of the FWHM of the 1331 cm^{-1} peak. Like the curve of figure 8, the FWHM does not depend on detailed deposition parameters and a line drawn through the data points is consistent with the value for natural diamond. The spread in the data points at the higher values of the FWHM could represent a saturation in the thermal conductivity similar to that which is possibly seen in figure 8.

That CVD diamond films may have a lower thermal conductivity than type IIa natural diamond has been suggested by Morelli et al[8]. Their data on the temperature dependence of diamond film thermal conductivity was consistent with phonon scattering at crystallite boundaries being an important effect in the films even at 300°K. This additional contribution to the thermal impedance of the films would act to lower the maximum thermal conductivity and shift it to higher temperatures. The data from figures 7-9 are consistent with this. Comparing films 10-N-83 and 10-N-107 in figure 5, shows that films of the same crystallite size can differ by a factor of two in thermal conductivity. This point is also illustrated by comparing 10-N-107 in figure 5 with 6-A-35 in figure 6. In this case films with similar thermal conductivities have film feature sizes which differ by a factor of 5 to 10. This lack of size effects is consistent with the discussion above if it is assumed, as seems reasonable, that boundary scattering effects will be important only in the films very similar in composition to natural diamond, i.e. important in those films of high Sp^3/Sp^2 or low FWHM. In films with more Sp^2 component, the thermal conductivity will be determined by by the amount of disordered carbon present in the film.

Conclusions

The thermal conductivity of CVD diamond films have been measured and correlated with the FWHM of the 1331 cm-1 peak of the Raman Spectrum and the ratio of diamond to disordered carbon as measured by Sp^3/Sp^2. These correlations are independent of the deposition technique or the deposition conditions suggesting that the FWHM and Sp^3/Sp^2 are indicative of the intrinsic diamond character of the film. No correlation with the film morphology was apparent.

A thermal conductivity of 12.3 W/cm-°C was measured at 117°C, the highest reported for thin CVD diamond films and nearly equal to that of type IIa natural diamond at the same temperature. However the data presented here is also consistent with a maximum thermal conductivity of 10-12 W/cm-°C due to boundary scattering of phonons in the 1μ-2μ crystallites typical of these films. Nonetheless, CVD diamond films can be fabricated with thermal conductivities twice to three times that of copper and over five times that of ceramics typically used in electronic packaging. These thermal characteristics in conjunction with their other unique properties make diamond films an excellent choice for the material of a new generation of electronic packages.

Acknowledgements

The authors would like to acknowledge Shari Yokota for assistance with the SEM and Raman analysis and Louise Nichols for help with sample mounting. Portions of this work was supported by the Air Force through the Wright Patterson Research and Development Center.

References

1. M. Peters, J.M. Pinneo, L.S. Plano, K.V. Ravi, V. Versteeg, and S. Yokota; SPIE Proceedings; San Diego, January 1988.
2. A. Sawabe and T. Inuzuka, *Appl. Phys. Lett.*, **46**,1985, pp. 146.
3. A. Sawabe and T. Inuzuka, *Thin Solid Films*, **137**, 1986, pp. 89.
4. Y. Hirose and Y. Terasawa, *Japanese Journal of Applied Physics*, 25 (6), June 6 1986, pp. 151.
5. V.P. Varnin, et al., *Sov. Phys. Dokl.*, **29** (5), 1984, pp. 419.
6. J.C. Angus and C.C. Hayman, *Science*, **241**, Aug. 19 1988, pp. 877-1016.
7. A. Ono, T. Baba, H. Funamoto, and A. Nishikawa, *Japanese Journal of Applied Physics*, **25** (10), Oct. 1986, pp. L803-L810.
8. D.T. Morelli, C.P. Beetz, and T.A. Perry, *J. Appl.Phys.* **64**, Sept. 15 1988, pp.3063-3066.
9. *Handbook of Physics and Chemistry, 52nd Edition*
10. Linda S. Plano and Fran Adar, Proceedings on the SPIE International Conference on Raman and Luminescence Spectroscopy in Technology, San Diego, August 1987.
11. Diane S. Knight and William B. White, *J. Materials Research*, 4 (2), Mar/Apr 1989, pp. 385-393.

Figure 1. Schematic diagram of a mounted sample.

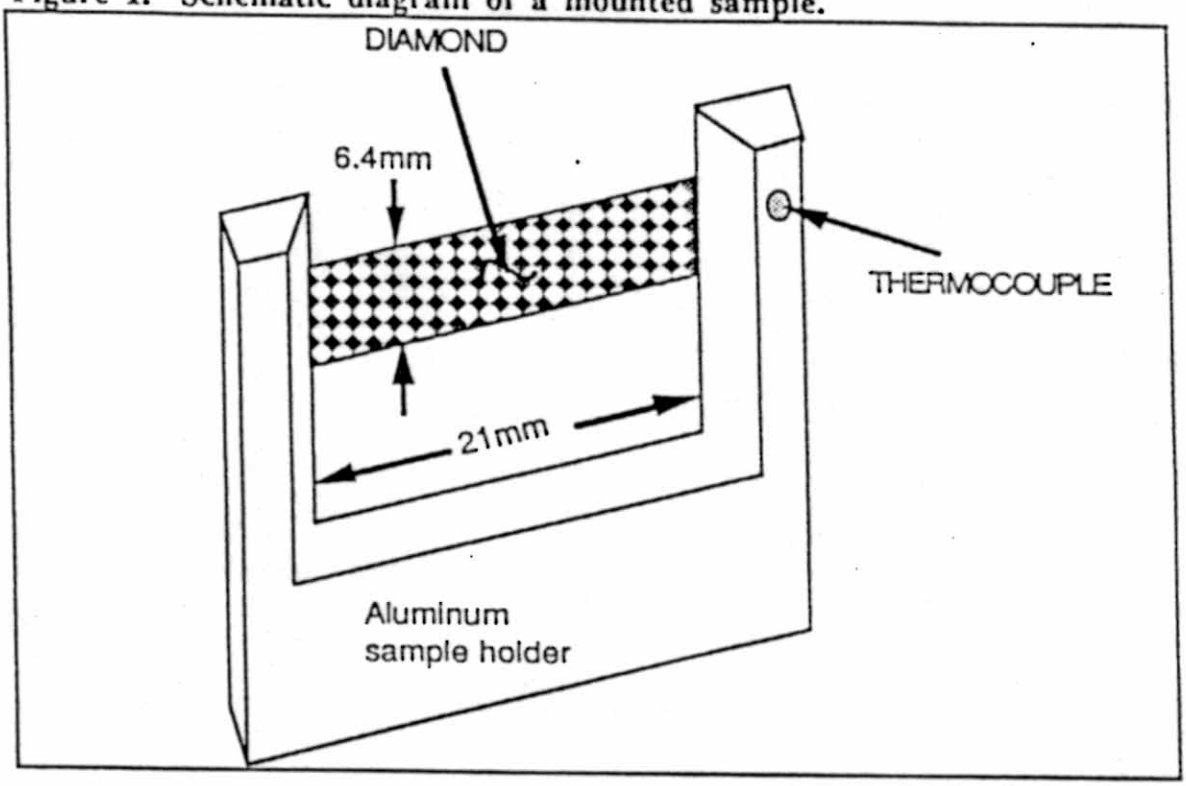

Figure 2. Schematic Diagram of the Measurment System

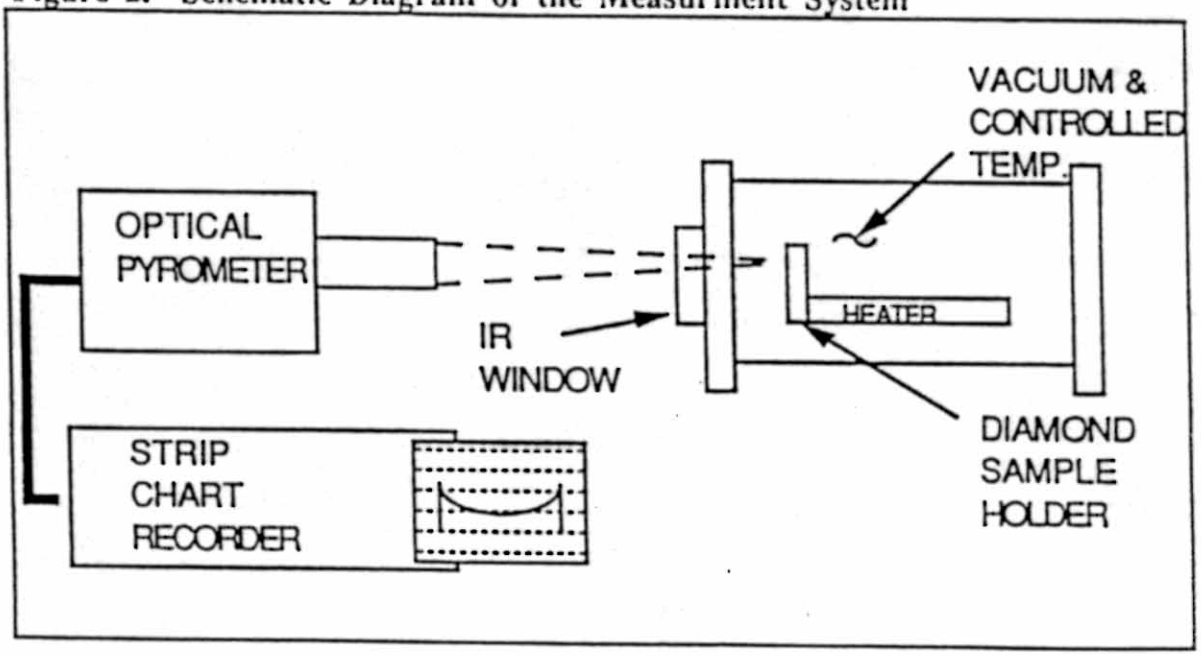

Figure 3. Raman Data for Diamond Films Deposited by Microwave PECVD

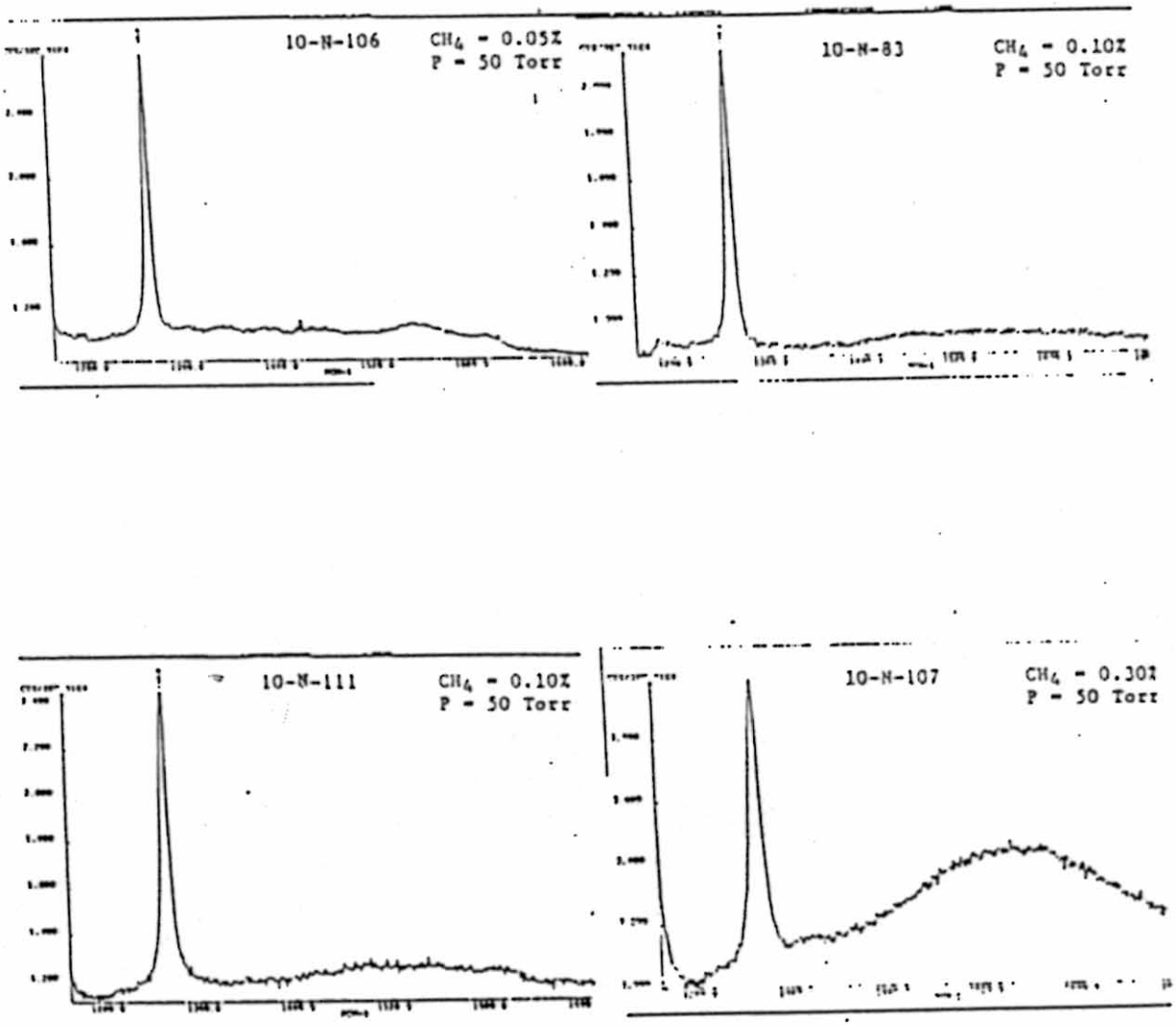

Figure 4. Raman Data for Diamond Films Deposited by D.C. PECVD

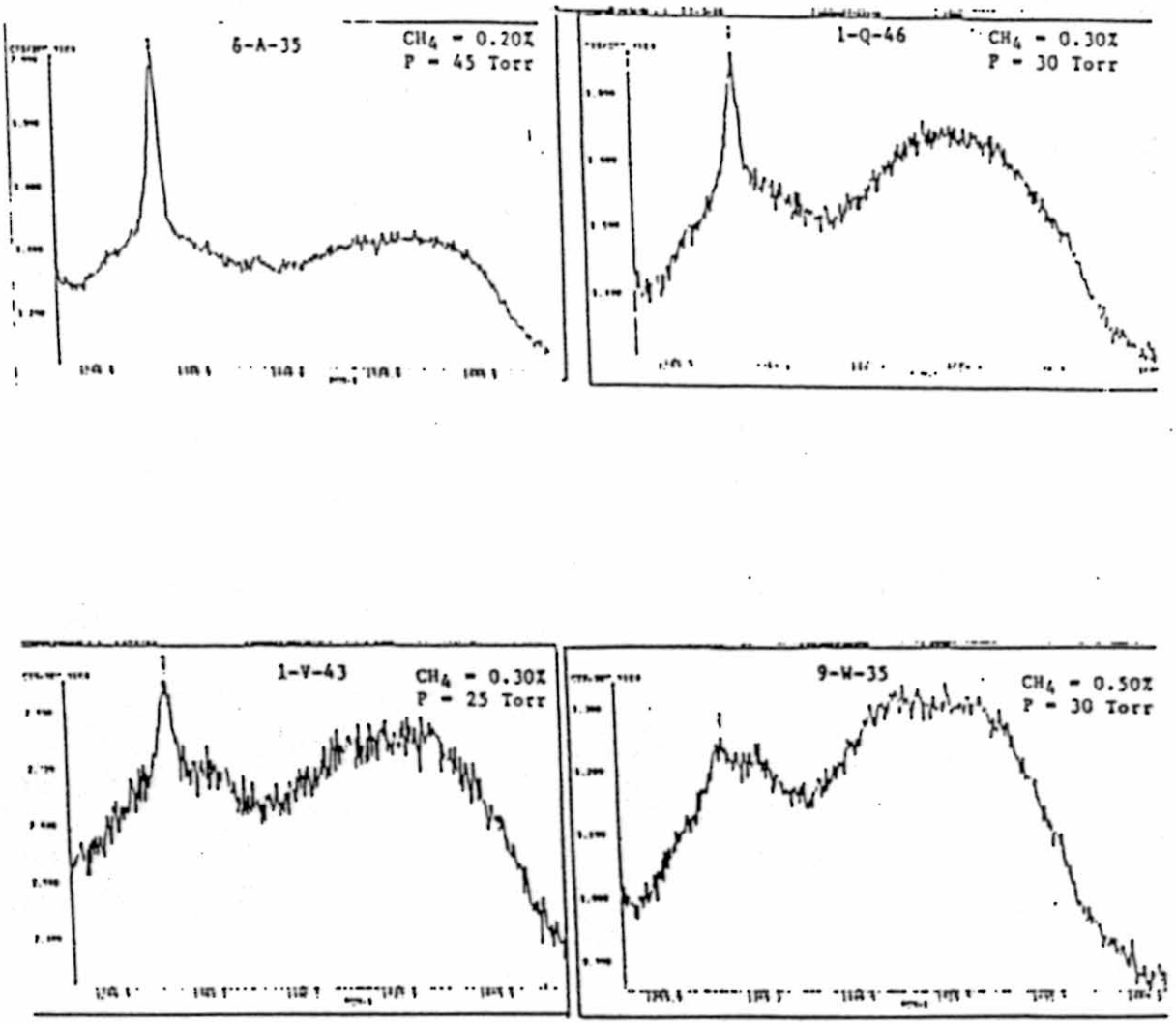

Figure 5. Surface Morphology of Diamond Films Deposited by Microwave PECVD

10-N-106

10-N-83

10-N-111

10-N-107

Figure 6. Surface Morphology of Diamond Films Deposited by D.C. PECVD

6-A-35

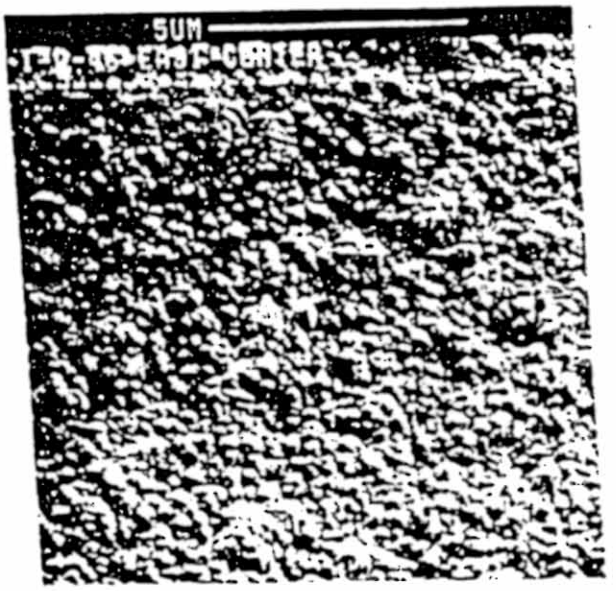

1-Q-46

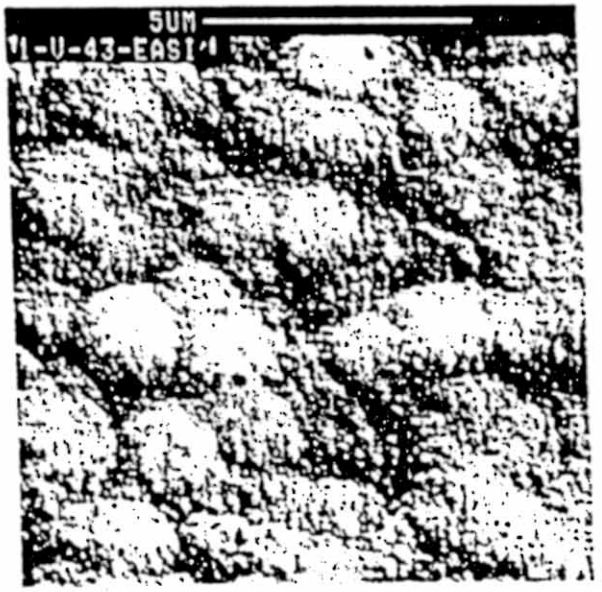

1-V-43

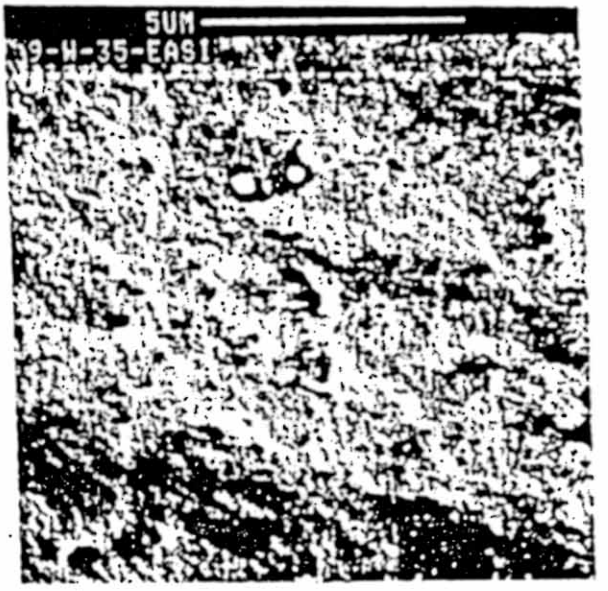

9-W-35

Figure 7. Thermal Conductivity vs. Methane Concentration

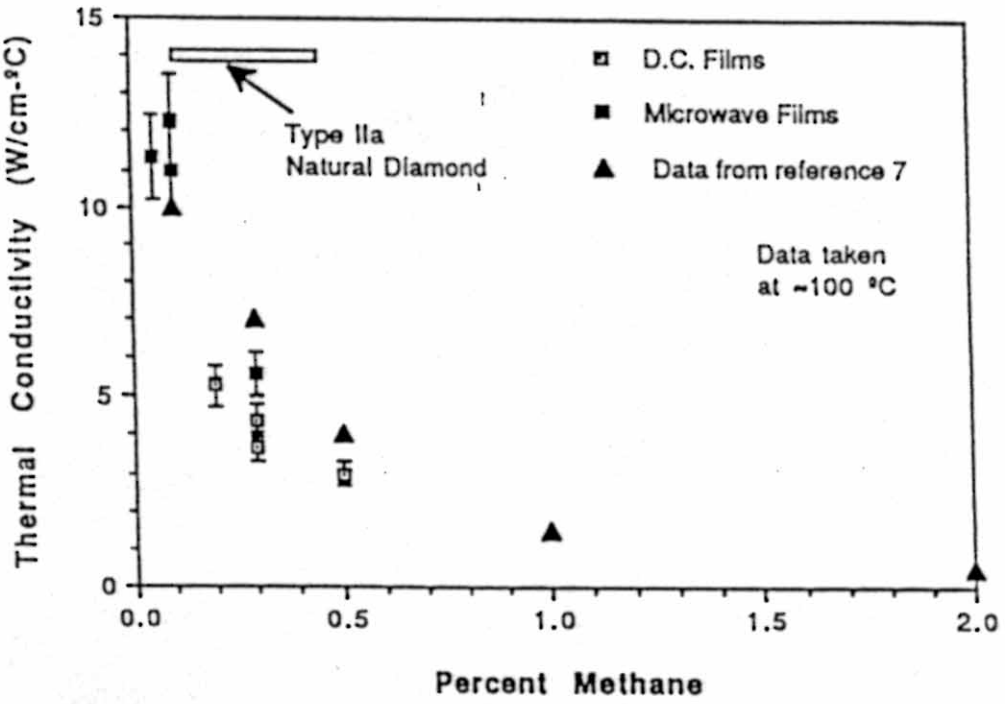

Figure 8. Thermal Conductivity vs. Sp^3/Sp^2

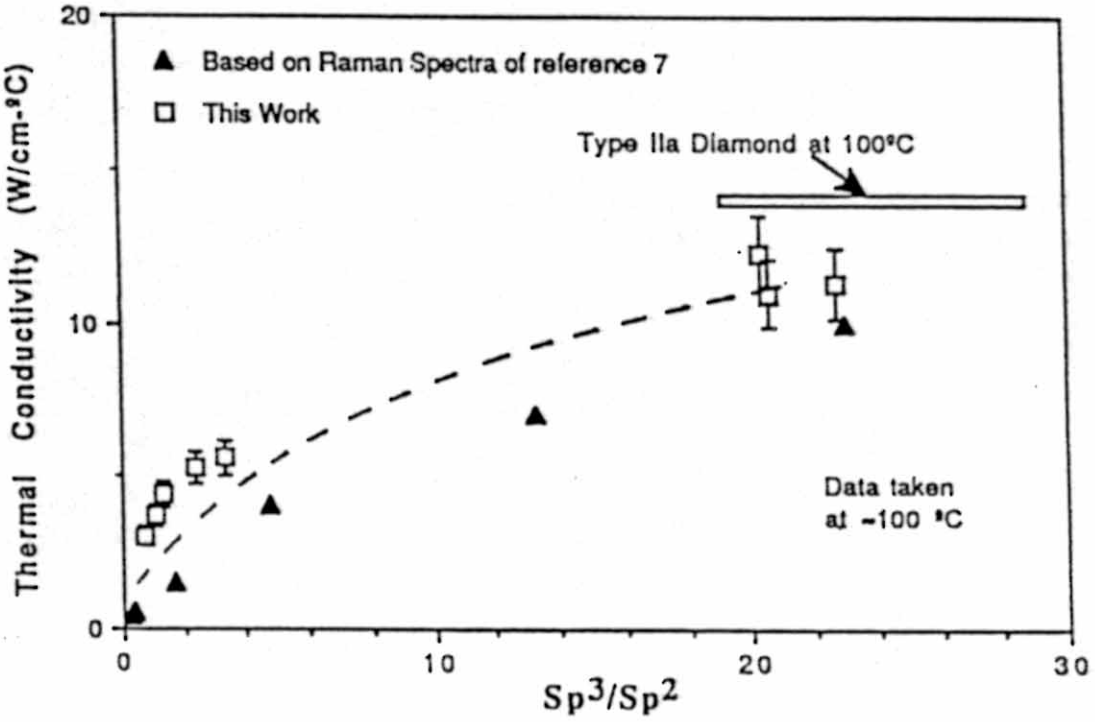

Figure 9. Thermal Conductivity vs. FWHM of the 1331 cm^{-1} Peak